Synthesis of 58S bioactive glass based on a novel methodology employing microwave technology

E. Cañas[1*], A. Borrell[2], R. Benavente[2], M.D. Salvador[2]

[1]Instituto Universitario de Tecnología Cerámica (IUTC), UniversitatJaume I (UJI), Castellón, Spain
[2]InstitutoUniversitario de Tecnología de Materiales (ITM), Universitat Politècnica de València (UPV), Valencia, Spain

Eugeni Cañas Recacha Telephone number: (+34) 964342424
Email: eugeni.canas@itc.uji.es Fax number: (+34) 964342425

Amparo Borrell Tomás
Email: aborrell@upv.es

Rut Benavente Martínez
Email: rutbmr@upvnet.upv.es

María Dolores Salvador Moya
Email: dsalva@mcm.upv.es

Abstract
The sol-gel method for bioactive glass synthesis offers advantages such as precise control over the chemistry, a straightforward way of modifying the composition and lower processing temperatures. However, longer processing times are required, increasing energy consumption.
The present work successfully produced 58S bioactive glass employing microwave technology and a two steps synthesis route, saving significant energy and time (76% and 99 % respectively) compared to conventional methods such as sol-gel and hydrothermal method, directly impacting on cost savings and competitiveness.
Microwave pressure played a key role: higher pressure led to lower content of residual nitrates and could reduce final processing temperature. This pressure dependence allows for precise control of the glass properties.The resulting glass closely resembled the characteristics and properties of the same glass produced by conventional methods, demonstrating the effectiveness of microwave technology. Moreover, the glass reacted positively with Simulated Body Fluid, indicating good bioactivity.

Keywords: 58S bioactive glass; Powders;Bioactivity; Microwave technology

1. Introduction

Due to the exceptional bioactivity exhibited by bioactive glasses, these materials find widespread utility across diverse applications, including not only replacement, regeneration and repair of hard tissues but also soft tissue regeneration and wound healing such as nerve regeneration, urinary tract or laryngeal repair among others[1].

Concerning the synthesis of these glasses, the most employed methods are the melt-quenching and sol-gel techniques[2,3]. The former yields glasses characterized by particles of low porosity texture, very low specific surface areas, and limited bioactivity, particularly evident in in-vivo assessments[4,5]. Conversely, the sol-gel method holds greater appeal for bioactive glass synthesis. It not only allows to operate at lower sintering temperatures but also offers greater versatility in modifying and controlling the composition of the resulting material, such as incorporating dopant metallic elements to confer specific functionalities, while minimizing impurities in the composition[3]. Moreover, glasses produced through this method exhibit heightened bioactivity due to their larger specific surface area, as a consequence of the high micro and mesoporosity of the particles obtained[4,5]. This porosity further allows for the production of more stable bioactive glasses, with SiO_2 content potentially reaching a molar percentage of 90%, all without compromising bioactivity[2,6].

Nevertheless, the sol-gel method demands lengthy material processing times, at times extending to weeks according to some researchers, resulting in substantial energy consumption. This has prompted a decade-long focus on refining the processing of solutions derived from the sol-gel method after the dissolution of the alkoxides and salts, with the aim of reducing the time required to obtain the desired material. Onealternative is the hydrothermal synthesis of glass using these solutions[7–10]. Once the feedstock is obtained, it is introduced into a sealed teflon reactor and heated to temperatures around100 - 200°C in an autoclave. Due to the sealed nature of the reactor, pressure exponentially increases as the temperature rises[8], expediting hydrolysis and condensation reactions. While this process is faster than the sol-gel method, it still necessitates approximately a minimum of 15 - 24 hours to complete these reactions in all studies conducted[7–10]. Furthermore, as it yields a glass rather than a crystalline phase, a gel forms which must undergothermal posttreatment exceeding 600°C in a conventional oven for several hours to stabilize the glass in order to

ensure the elimination of nitrates and organics, and to introduce alkaline and alkaline-earth elements into the glass network.

Therefore, as an innovative alternative for processing precursor solutions, this study proposes the synthesis of bioactive glass powder for thermal spray applications using microwave-based processing technologies. Microwaves (MW) represent electromagnetic energy associated with electromagnetic fields within the wavelength range of 300 MHz to 300 GHz[11,12]. When directed at the surface of a material or element, it gradually penetrates the material being transformed into heat energy. It is important to note all microwave radiations are allowedfor heating materials, but only the so-called Industrial, Scientific and Medical (ISM) frequencies, 915 MHz and2.45 GHz, are used[11,12].

Microwave processing holds significant promise, owing to its potential applications in ceramic material processing. It facilitates rapid, volumetric, and uniform heating, eliminating selective surface heating[13]. Additionally, it offers energy efficiency, requiring minimal energy consumption to attain low to moderate working temperatures, resulting in higher yields and shorter preparation times, reduced processing costs, finer and more uniform particle size distribution, and enhanced purity[11–13]. As documented in the literature, the study of this technology for materials processing has experienced exponential growth in recent times[14]. Microwave technology is widely employed in the synthesis and sintering of various advanced ceramic materials such as simple oxides (for example alumina or zirconia), complex oxides (like magnesium aluminate, yttria-partially stabilized zirconiaor zirconium titanate) or bioceramics (including hydroxyapatite and calcium phosphates)[11,12,15].

Hence, the objective of this study is to synthesize for the first timebioactive glass powders with well-defined properties and compositions using only microwave technology. The synthesis process involves two stages: an initial stage employing a high-pressure, low-temperature microwave digester, where the solution rapidly undergoes hydrolysis and condensation processes, resulting in an aged and dried gel. This is followed by a second, even faster stage in which a single-mode microwave equipment, designed with a maximum electric field, operating at ambient pressure and low temperature is used to stabilize the gel and directly produce the desired glass.

2. Materials and methods

2.1. Starting material

The working composition chosen is that ofthe well-known bioactive glass 58S (58% SiO_2, 33% CaO and 9% P_2O_5,in wt%). Aqueous precursor solutions,with a total precursor concentration of 4 M (4 mol of precursors per litre of solution), were preparedand used as starting material.Derived from the desired composition, and according to literature related to the development of the glass 58S by the sol-gel method[16–18], tetraethyl orthosilicate or TEOS ($C_8H_{20}O_4Si$ synthesis grade, Merck, Germany), triethyl phosphate or TEP ($C_6H_{15}O_4P$ synthesis grade, Merck, Germany) and calcium nitrate tetrahydrate ($Ca(NO_3)_2{\cdot}4H_2O > 99\%$, VWR Chemicals, USA)were selected as sources of SiO_2, P_2O_5 and CaO, respectively.Moreover, nitric acid (HNO_3, Tritripur, Merck, Germany)was used as catalystwith the aim of hydrolysing the alkoxidesTEOS and TEP, since both are not miscible in water.

The procedure followed to prepare the starting materialinvolved, first, preparing an acidic dissolution in water with a concentration of 0.2 M. Then, the corresponding amount of TEOS was gradually added, ensuring it is done drop by drop and under constant magnetic stirring. After all the TEOS has been added, the mixture was left to stir for a minimum of 30 minutes until full clarification.Next, a similar procedure is followed with the remaining two reagents,

starting with the addition of TEP and then calcium nitrate. Once calcium nitrate has been added, the solution is left stirring for an hour instead of 30 minutes to ensure complete dissolution of this last reagent and to complete the hydrolysis.

Concerning the amount of the reactants, first the desired final oxide concentrations are first converted into molar ratios. Subsequently, leveraging the stoichiometry of the precursor reactions (according from literature [19]), the exact quantities of each starting material needed to yield the targeted glass oxides are calculated. Then, once the amount of each precursor is known, a molar ratio water to TEOS of 6 was considered in order to achieve the total concentration of precursors of 4 M.

2.2.Synthesis of bioactive glass

From the precursor solutions developed in the previous section, bioactive glass powders are synthesized using microwave technology, following a two-stage process.

The first stage, can be considered a pre-treatment of the material before its processing in the microwave furnace. In this stage, gelation of the solution, agingof the gel and drying of thexerogel were carried out in a microwave digestor system (Ethos One, Milestone Srl, Italy)only in one experiment, using teflon containers capable of withstanding high pressures. After solution preparation, the liquid material was placed inside the teflon containers and the whole were placed inside the digestor system. Tests were performed operating at only 300 W of power, employing a heating rate of 25^{o}C/min and a dwell time of 40 minutes. In this step,two temperatures were studied, with each temperature corresponding to a specific pressureas shown in Table 1.

Table 1. Temperature and its corresponding pressure for each experiment performed at the first step of synthesis

Sample reference	Temperature (^{o}C)	Pressure (bar)	Dwell time (min)
Glass 1 (G1)	170	18	40
Glass 2 (G2)	190	35	40

Subsequently, for each temperature-pressure tested, the resulting xerogel was dry crushed using an agatemortar to obtain a powder, where in a second stage of synthesis, this glass powder is stabilized using a single-mode microwave equipment.

For that purpose,a custom experimental single mode microwave system operating in the TE_{111} mode with a resonant frequency of 2.45 GHz was selected as the heating cell for microwave[20]. The samples were placed within a cylindrical cavity, which is automatically adapted to maximize microwave absorption by the material, enabling precise control over heating rates, stabilisation temperature and residence time. In addition, with the aim of better control of the heating rate and microwave absorption, during the whole process the temperature of the sample surface was continuously monitored using an infrared pyrometer that had been calibrated in advance for the desired temperature range. Both powder samples (G1 and G2) were subjected to the same stabilising firing cycle in the microwave furnace, always at the lowest possible temperature of stabilisation, which is determined from a thermogravimetric analysis (detailed later). The rest of parameters used were 700 W of power, heating rate of 60 ^{o}C/min,air atmosphere, 10 minutes of stabilisationat the maximum temperature and free cooling. The total cycle time was 25 min.These specific conditions were chosen based on prior investigations conducted within the research group.

Both powders were introduced into the microwave cavity with the same experimental set up as depicted in Figure 1. As it can be seen, the powder material is placed into an alumina crucible and the whole is suspended in the airinside a silica vessel onto a box of

alumina.Except for the powder under study, all the other materials aretransparent to microwaves, and thus, they do not have any effect on the different components of the set up.

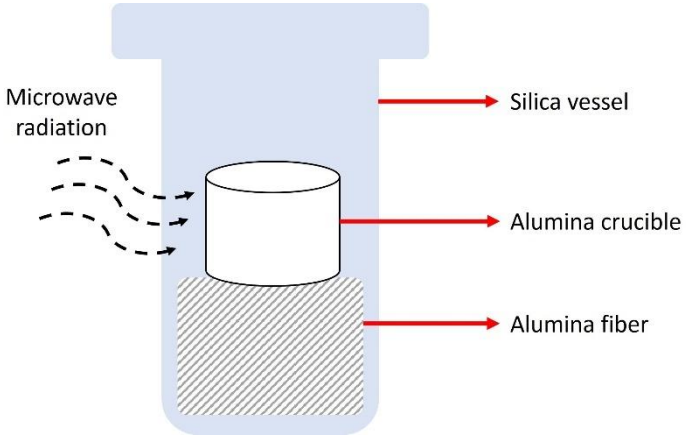

Figure 1. Experimental set up utilized to heat the xerogel powders in the microwave cavity

2.3.Characterisation of the synthesised glasses

2.3.1. Thermogravimetric analysis

Thermogravimetric analysis (TGA) was performed in order to assess the stabilisation temperature of the synthesised glass by means of a thermogravimetricanalyser (TGA Q50, TA Instruments,USA).Powder samples from the first synthesis step were placed in a platinum crucible and heated in air atmosphere from room temperature until 750 ^{o}C at a heating rate of 10 ^{o}C/min. Prior the test, the samples were kept in an oven at 80 ^{o}C to avoid the adsorption of ambient humidity, since these materials are highly hygroscopic.

2.3.2. X–ray diffraction analysis

The amorphous or crystalline character of the glass powder after both synthesis steps was determined by X–ray diffraction (XRD). The different spectra were acquired througha diffractometer (Theta–theta D8 advance diffractometer, Bruker, Germany) employing Cu Kα radiation (λ = 0.154183 nm),a power of 30 kV and 40 mA, and data were collected over a range of 2θ between 5^{o} and 80^{o} using a step size of 0.02^{o}.

2.3.3. Scanning electron microscopy

The morphology of the glass particles after the second step of synthesis was observed by means of scanning electron microscopy (SEM).Micrographs of the synthesised powders were taken at low vacuum, 20 kVand different magnifications under the backscattering electrons signal, employing a field emission gun environmental scanning electron microscope (Quanta 200FEG, FEI Company, USA). Prior to the observation, the powder samples were carbon coatedby sputtering in order to obtain conductive samples.

2.3.4. Energy–dispersive X–ray microanalysis

Energy–dispersive X–ray microanalysis (EDX) was employed with the aim of determining the elemental composition of the glasses after the second step of synthesis. Through an X-ray spectrometer and an energy detector (Genesis 7000 SUTW, EDAX, USA) coupled to the SEM, spectra of differentgroups of particles from several zones of the sample holder were taken at the same conditions as the SEM micrographs were done.

2.3.5. BET specific surface area

The specific surface area (S_{BET}) was determined using the Brunauer-Emmett-Teller (BET) method from adsorption isotherms according to the ISO 9277:2010 standard and employing an adsorption analyser (TriStar 3000, Micromeritics, The USA) with nitrogen gas as the adsorbent.The adsorption constant (C), which reflects the strength of the interaction between the adsorbate (nitrogen) and the adsorbent (sample surface), was also determined from the analysis.According to the standard, the C parameter should fell within the recommended range of 50-200 for reliable BET analysis.Prior to the analysis, samples were degassed. This involved oven drying at 110 °C for 2 hours followed by a nitrogen stream purge at 150 °C.

2.3.6. Fourier transform infrared spectroscopy

Fourier transform infrared spectroscopy (FTIR)was performed to determine the functional groups present in the glass after the stabilisation step by means of a spectrometer (FT/IR–6200, Jasco Inc., Japan)equipped with an ATR Pro ONE with diamond crystal (Jasco Inc., Japan). The glass powders were analysed in transmittance mode for the range comprised between 1400–400 cm^{-1} with a resolution of 4 cm^{-1}.

2.3.7. Invitro test

Invitro test of the developed glasses was performed by means of soaking the powders in Simulated Body Fluid (SBF) according to a standard protocol[21].

First, the SBF was prepared following the method of Prof. Kokubo [22]. Then, 60 mg of glass powder were soaked in 40 mL of SBF in sealed polyethylene vessels, and the vessels were placed inside a water bath at 36.5 ± 0.5 °C. The amounts of glass powder and SBF were determined according to the 1.5 mg of glass per mL of SBF ratio stablished at the followed protocol [21].Different soaking times were studied, i.e., 1and 7 days, and for each soaking time, three different powder aliquots of each synthesised glass were tested.

After each soaking time, the powders were removed, gently rinsed with distilled water and dried overnight in an oven at 80 ^{o}C. After that, the nucleation and growth of hydroxycarbonate apatite (HCA) was monitored for each time. SEM was used to observe the surface morphology of the particles. For that purpose, micrographswere taken at high vacuum and 5 kV under the secondary electrons signal.The chemical composition of the surface was studied by EDX (same conditions than SEM micrographs but increasing the energy to 20 kV) and the presence of HCA was analysed by XRD (same conditions as in section 2.3.2).

3. Results and discussion

3.1.First step of synthesis. Before glass stabilisation

In this section, the results obtained in the first stage of the experimental procedure, which focused on the initial synthesis of glass using a microwave digestor system, are presented. This initial phase holds crucial importance as it establishes the characteristics of the material used for the formation of bioactive glass that will subsequently be developed in the second stage.

Figure 2, shows a picture of each xerogel powder before the stabilisation of the glass matrix. Contrary to what was expected, the powders show an orange shade, which is more intense when the pressure reached during the experiment was higher.

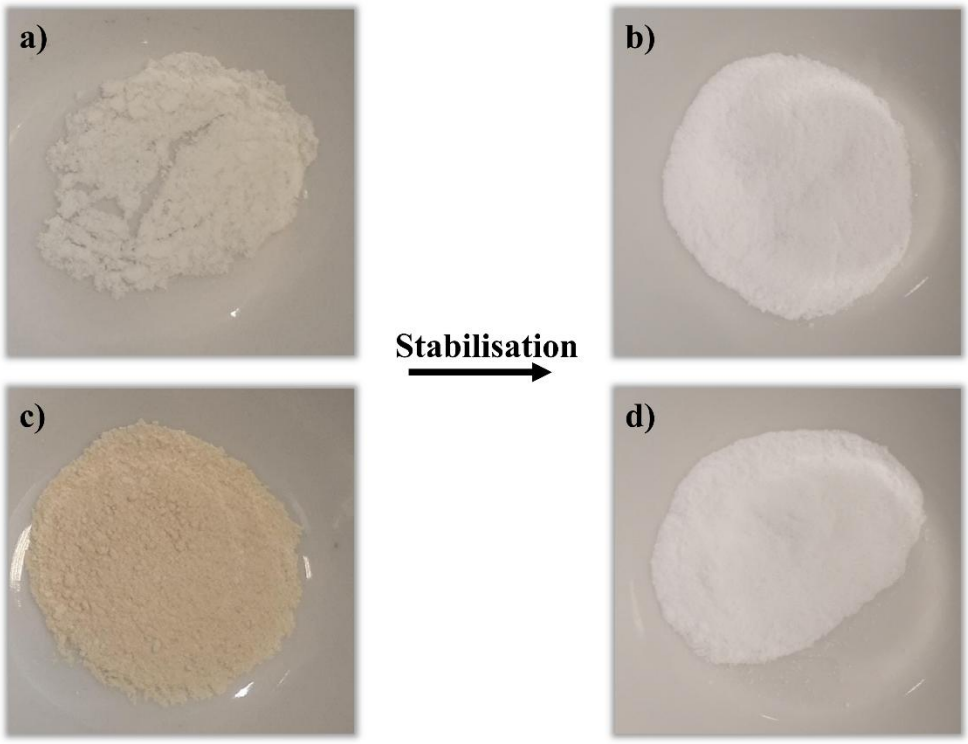

Figure 2. Images of the xerogel powders before and after thermal stabilisation. a) and b) G1 (170ºC-18bar-40min) before and after stabilization, respectively, c) and d) G2 (190ºC-35 bar-40 min) before and after stabilization, respectively

After analysing both powder samples with XRD (Figure 3), in all cases it can be appreciated that the result of the first step is a mixed material which combines an amorphous phasewith the presence ofsome crystalline peaks of different nitrogen-based organic compounds, i.e.,tetracycline hexahydrate ($C_{22}H_{24}N_2O_8 \cdot 6H_2O$, PDF: 39-1985), psilocybin methanolate ($C_{12}H_{17}N_2O_4P \cdot CH_4O$, PDF: 30-1903) and riboflavin tetrabutyrate ($C_{33}H_{44}N_4O_{10}$, PDF: 44-1609). This fact contrasts with the literature[23], where a fully crystalline spectrum with characteristic peaks of only calcium nitrate is obtained.The development of these organic compounds, which should be the responsible of the colouring of the powder, may be due to the pressure to which the material is subjected in the microwave digestor system, which promotes the reaction between the ethanol from the hydrolysis of TEOS and TEP, and the nitrates from the solubilisation of calcium nitrate. Moreover, as happens with the shade, a clear effect of pressure can be seen, i.e.,the higher the pressure, the higher the formation of these compounds, as the presence and intensity of the peaks is higher for glass 2 (G2), which reaches a higher pressure (35 bar).

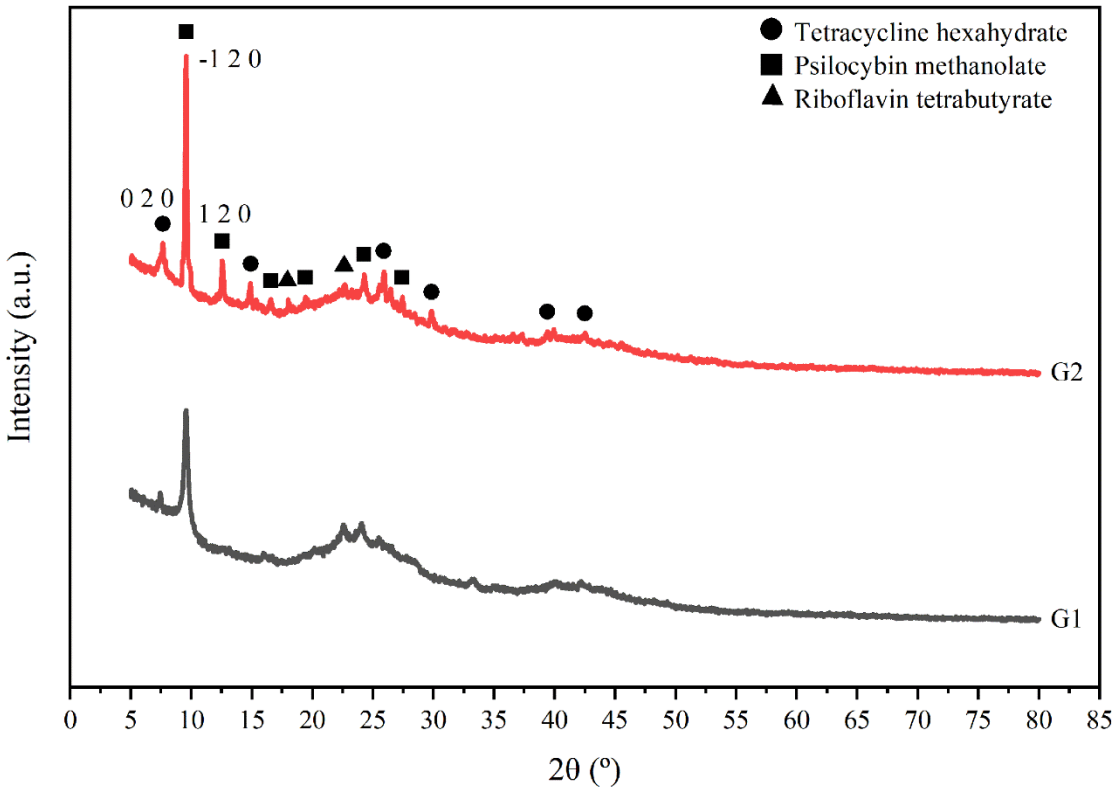

Figure 3. XRD spectra of the two xerogel powders, G1 and G2, after the first synthesis step

Finally, a thermogravimetric analysis was conducted on the xerogel powders. Figure 4, shows the weight loss curve and the derivative curve along with the peak temperatures while the Table 2, shows the total weight loss percentage.

As illustrated in Figure 4, both glasses exhibit three clearly defined weight loss regions within temperature ranges of 25-150°C, 150-350°C, and 350-600°C which are quite consistent with otherworks[10]. Furthermore, beyond 600°C, no further weight loss is observed and both glasses end up having lost approximately the same amount (Table 2). Hence, this temperature is selected as the stabilisation point for both glasses.

According to literature[10], the first region is assigned to the elimination of the physically adsorbed water and residual alcohol, the second zone is attributed to the desorption of chemically adsorbed water and the last one, with the highest weight loss, to the decomposition of the nitrates from the salt precursors. In this work, the same three phenomena take place for both glasses, but coupled with the elimination of the nitrogen-based organic compounds in the first two regions between 100 and 250 ºC. Therefore, some nitrates are removed at lower temperatures than in the conventional methods (sol-gel and hydrothermal) resulting in higher weight loss percentages in the first two regions and lower in the third one. This fact could facilitate the stabilisation of the glass.

When glasses G1 and G2 are compared, it can be seen that the profiles in Figure 4are quite similar. Nevertheless, the effect of the pressure reached inside the microwave digestor it is also noticeable when paying attention to both the derivative curves in Figure 4 and Table 2. It has been noted that the peak temperatures within each weight loss region exhibit remarkable similarity, but there are discernible differences in the peak intensities, particularly within the second and third regions. As previously mentioned, G2 glass attains higher pressures, resulting in the generation of a greater quantity of nitrogen-based organic compounds.

Consequently, the peak in the second region is notably more pronounced for G2 glass, while the peak in the third region is comparatively less intense. This observation aligns with the data presented in Table 2, which indicates higher losses in the second region and lower losses in the third region for G2 glass.

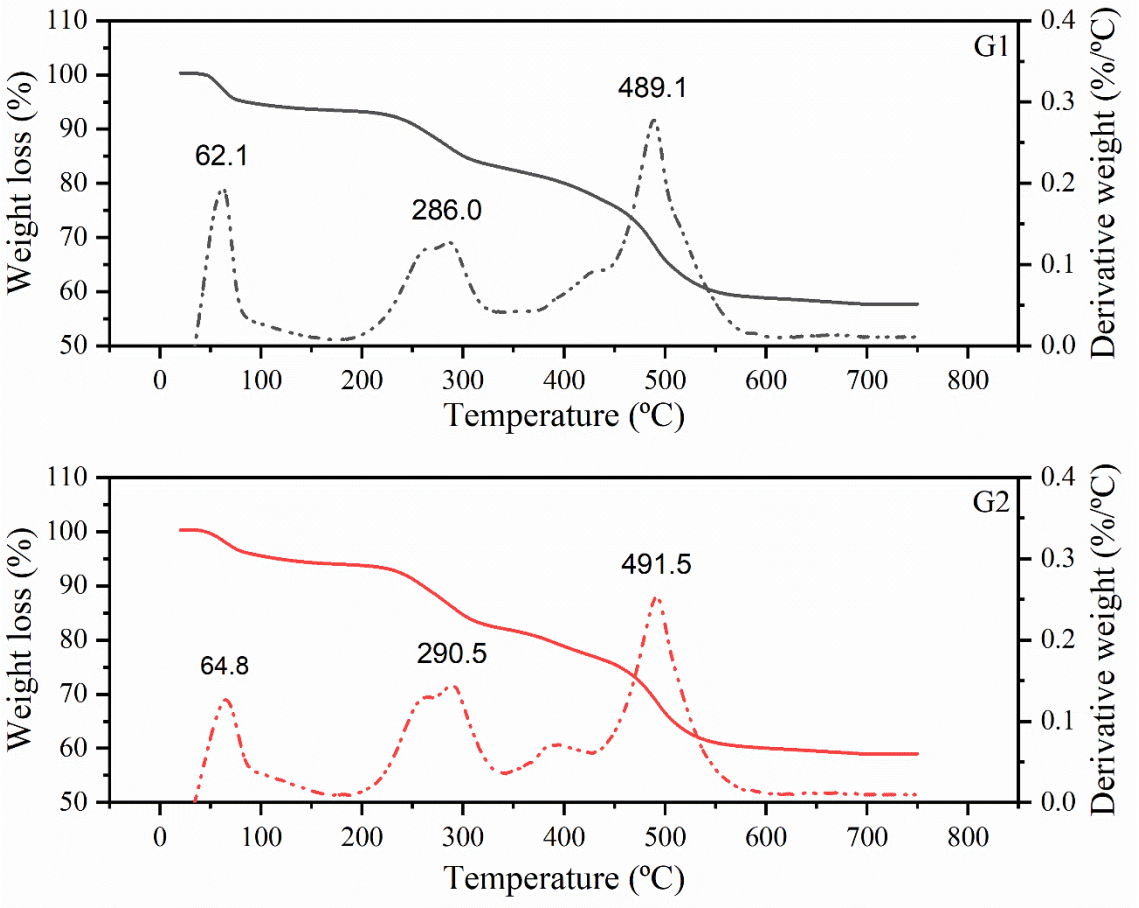

Figure 4. Weight loss (continuous curve) and its derivative (dotted curve) in function of temperature for each xerogel powder

Table 2. Percentage of weight loss for the three temperature ranges

Sample reference	25 - 150 ºC	150 - 350 ºC	350 - 600 ºC	Remaining
G1 (170 ºC - 18 bar)	6.4 %	12.2 %	23.2 %	58.2 %
G2 (190 ºC - 35 bar)	6.1 %	15.3 %	20.5 %	58.1 %

Last but not least, by the utilisation of a microwave digestor (300 W and 40 min), a reduction of 75% in energy (W) and 98% in time consumption(h) was accomplished compared to a typical sol-gel procedure which usually involves using an oven, with an average energy consumption of 1200 W, for approximately 5 days to perform gelation, aging, and drying of the solution.

3.2.Second step of synthesis. Glass stabilisation

After stabilising both glasses at 600 ºC in the microwave cavity, a powder material is still obtained with an angular, irregular and non-spherical shape, typical of a ground glass material,as can be seen for both glasses in Figure 5. Both glasses look very similar and are composed of a mix of particles with a widesize distribution.

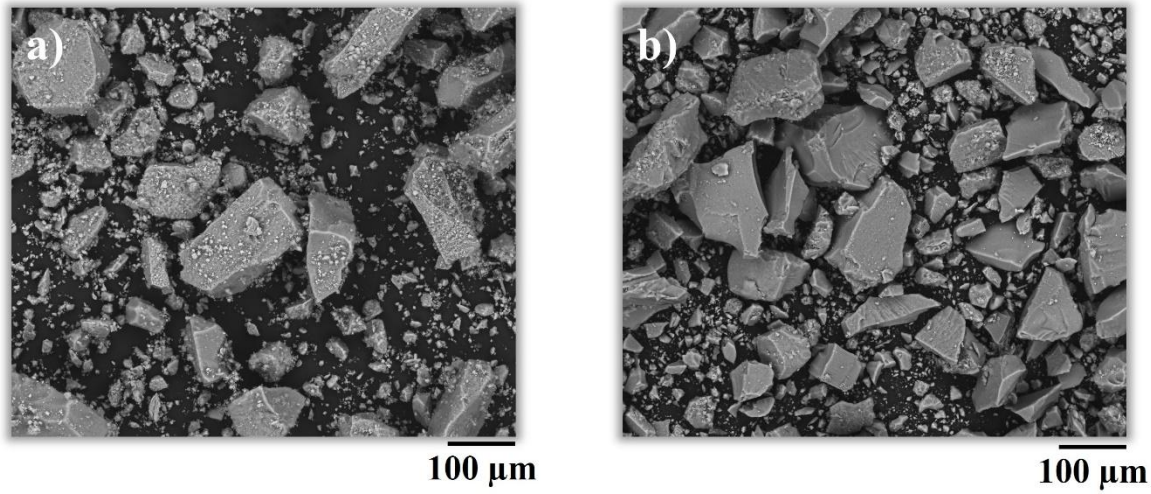

Figure 5. Micrographs of the glass particles after second synthesis step. a) G1 (170 ^{o}C - 18 bar), b) G2 (190 ^{o}C - 35 bar)

Table 3 shows the composition of both glasses, which is quite similarto the composition of the nominal glass 58S. Only a slight difference on the phosphorusoxide content can be appreciated, since this compound volatilises easily from the particle surface, as has been seen in other work [24].

Table 3. Compositions of the nominal bioactive glass 58S and both glasses after the second synthesis step

Composition (wt%)	SiO_2	CaO	P_2O_5
Bioactive glass 58S	58.0	33.0	9.0
G1 (170 ºC - 18 bar)	58.4 ± 0.9	33.9 ± 0.5	7.7 ± 0.3
G2 (190 ºC - 35 bar)	58.5 ± 0.9	33.6 ± 0.8	7.9 ± 0.3

On the other hand, following the stabilisation process, entirely amorphous glasses were obtained, as demonstrated in Figure 6, where the spectra of both glasses showed no signs of crystalline peaks. This a priori confirmation indicates that the stabilisation process was executed correctly, as all the organic phases present in the glass after the initial synthesis stage (Figure 3) were completely eliminated by thermal decomposition. In fact, as it can be seen in Figures 2b and 2d both glasses have lost its orange shade and become completely white powders.

Concerning the specific surface, the values of the synthesised glasses are shown in Table 4 with values from literature about sol–gel derived 58S bioactive glass [25]. It can be appreciated that both synthesised glasses present a surface area quite similar and within the range of the nominal glass. Moreover, the synthesised glasses also display high adsorption constants (C), indicating strong interactions between the gas molecules being adsorbed and the surface of the solid material[25].

Table 4. Specific surface area ofsol–gel derived bioactive glass 58S and glasses after the second synthesis step

Composition (wt%)	Specific surface area (m^2/g)	Adsoption constant (C)
Sol–gel derived 58S bioactive glass [25]	126 – 165*	157 – 243

G1 (170 ºC - 18 bar)	139	125
G2 (190 ºC - 35 bar)	130	128

*Depending on the mean particle size

Finally,the structural assessment of both glass variants was performed via FTIR, and the outcomes are visually presented in Figure 7. According to the existing literature[4,26,27], both glasses showcased the characteristic bands associated with 58S bioactive glass. Notably, no signals of organic compounds or undesired phases were detected, thereby affirming the accurate synthesis of the intended glass.

Specifically, distinct features were observed in the spectra, including a broad peak at approximately 450 cm^{-1}, corresponding to the Si-O-Si rocking vibration, and a wide peak at around 800 cm^{-1}, signifying the Si-O-Si bending vibration. Additionally, two transverse optical resonant modes of silicon were discerned: a sharp peak at approximately 1030 cm^{-1} and a broad shoulder at roughly 1220 cm^{-1}, corresponding to TO_1 Si-O-Si and TO_2 Si-O-Si stretching vibrations, respectively. Furthermore, given that this research investigates a silicate glass modified through the incorporation of alkaline-earth elements, a visible broad band at approximately 940 cm^{-1}, corresponding to the Si-O-NBO stretching mode, was observed. The inclusion of phosphorous in the glass composition was also evident, as significant vibrations stemming from phosphate groups became apparent. This included a broad shoulder at around 1100 cm^{-1}, linked to the asymmetric P-O stretching vibration, and peaks at approximately 570 and 600 cm^{-1}, corresponding to P-O bending vibrations of PO_4^{-3}. The latter two peaks were attributed to an initial interaction of the particle surfaces with ambient moisture, leading to the development of an amorphous calcium phosphate thin layer[4].As a result of this layer, a minor shoulder at approximately 860 cm^{-1} emerged, which corresponds to C-O bending vibrations originating from CO_3^{-2}.

Despite having a similar spectrum, when comparing both glasses, the peaks are more sharply defined for G2 glass, suggesting that probably its structure is better developed.As mentioned above, since both glasses have undergone the same stabilisation process, this difference could be due to the pressure difference reached into the microwave digestor.

Last of all, stabilising the glass with a single-mode microwave equipment (700 W and 25 min) yielded a glassy material with the desired properties and characteristics, while significantly reducing the energy (W) and time consumption (h) by 77% and 92%respectively, compared to a conventional sol-gel procedure which usually involves using an electric furnace with an average energy consumption of 3000 W, for approximately 5 h to stabilise the glass.

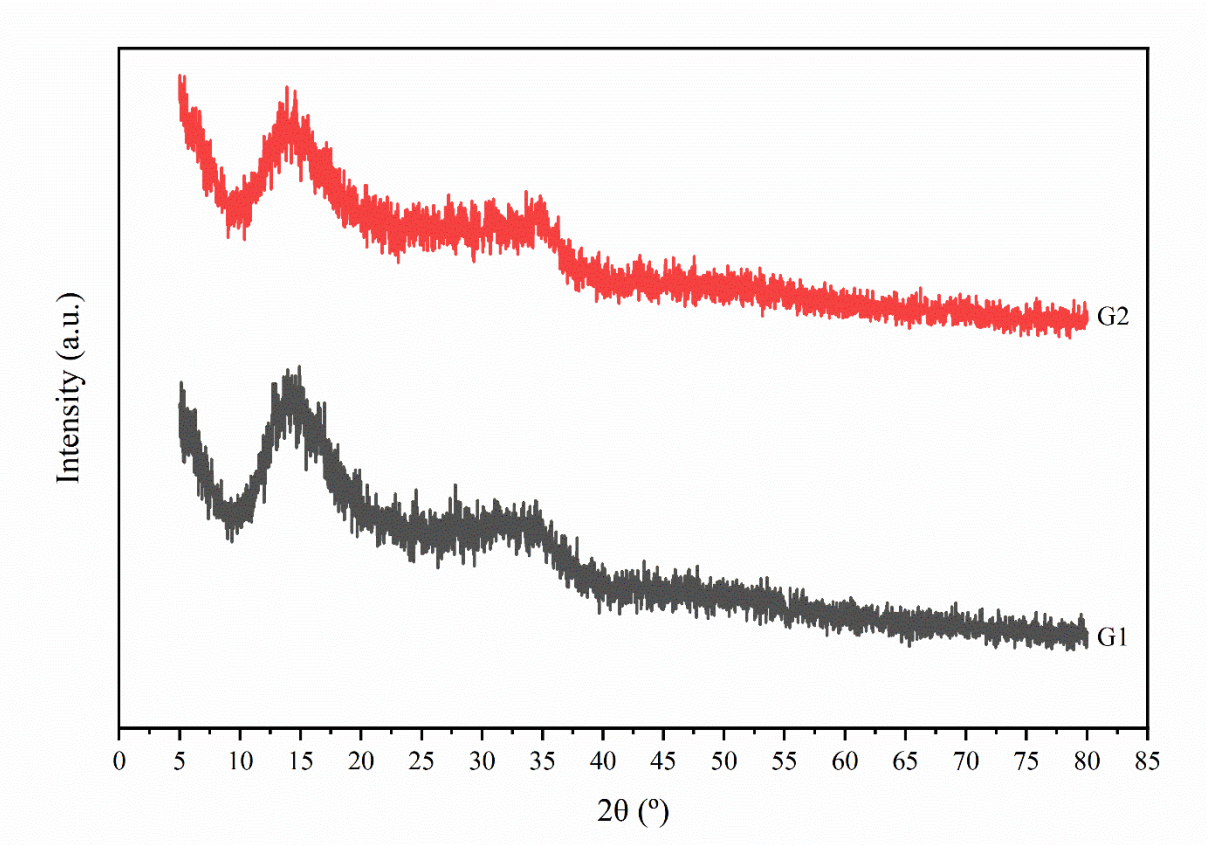

Figure 6. XRD spectra of the synthesised glasses after the second synthesis step.

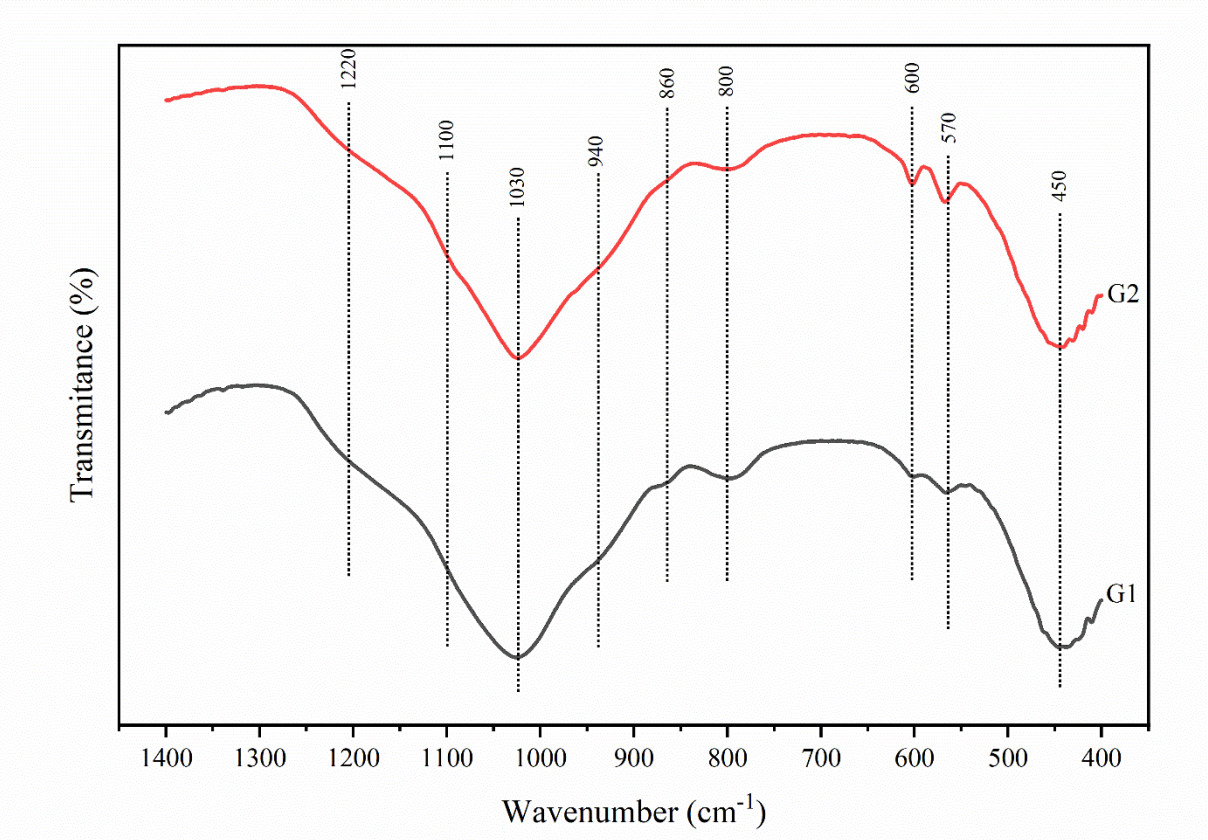

Figure 7. FTIR spectra of both glasses after the second synthesis step

3.3.Invitro characterisation

To analyse the ability of hydroxycarbonate apatite (HCA) to nucleate on the surface of the glass particles, which could be considered as a preliminary estimation of the bone-bonding ability of the synthesised glasses[28,29],after SBF the surface of the particles was analysed by means of SEM and EDX. Figure 8, shows the micrographs of G1 and G2 powders before and after soaking in SBF and Figure 9, show the EDX spectra of G1 powder for each soaking time (spectra for G2 is mostly the same).Despite the differences in pressure during the first step of synthesis, both glasses behave quite similar, since after a day of immersion in SBF, it is possible to observe the formation ofsilica gel layers on the particles of both glasses as a result of the ion exchange process, in which the glass leaches cations (Ca^{+2}) and receives protons (H^{+}) from the SBF. Subsequently, after 7 days of immersion in SBF, due to the migration of carbonate (CO_3^{-2}) and phosphate (PO_4^{-3}) ions from the SBF, along with calcium ions (Ca^{+2}) migrating from both the SBF and the interior of the particle, they combine on the silica gel layer, nucleating and forming a thin layer of carbonated hydroxyapatite[30], as illustrated in Figures 8c and 8f.

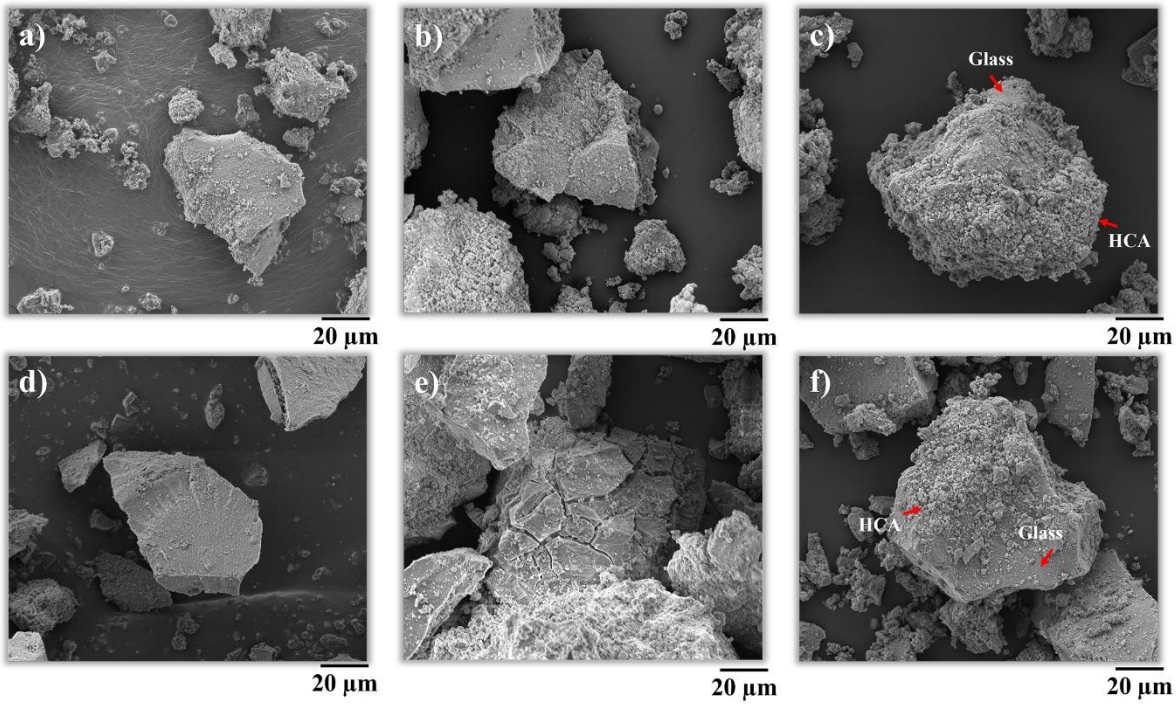

Figure 8. SEM micrographs of G1 and G2 glasses before and after soaking in SBF. a) G1 before soaking, b) G1 after 1 day in SBF, c) G1 after 7 days in SBF, d) G2 before soaking, e) G2 after 1 day, f) G2 after 7 days in SBF

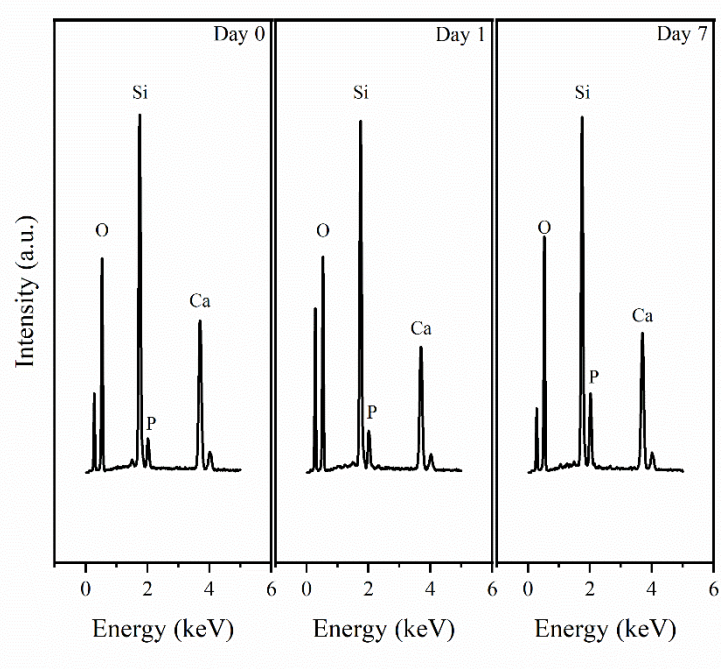

Figure 9. EDX spectra of the G1 glass after each soaking time in SBF

Indeed, all of the aforementioned points can be confirmed by examining the EDX spectra. In these spectra, it is evident that when transitioning from 0 to 1 day, the signal intensity of the calcium peak decreases (as a result of leaching). Conversely, when moving from 1 day to 7 days, both the intensity of the phosphorus peak and the calcium peak show a significant increase, indicating the formation of a calcium phosphate layer, in accordance with the described process[28,29]. Nevertheless, when comparing with the literature[4,10,23], the powders synthesized in this study do not exhibit as high of a bioactivity as the nominally 58S glass obtained through the sol-gel or hydrothermal methods. This could be attributed to the relatively short stabilization time used (10 minutes), which may not allow for the complete incorporation of calcium into the glass network, thus reducing the bioactive capacity of the glass as it remains on the surface and is quickly released upon immersion of the powder in SBF.

Despite the aforementioned limitations, it is possible to assert that the powders synthesized in this study do possess bioactivity. This is substantiated by the presence of carbonatedhydroxyapatite, as confirmed after 7 days of immersion through X-ray diffraction (DRX), as depicted in Figure 10.

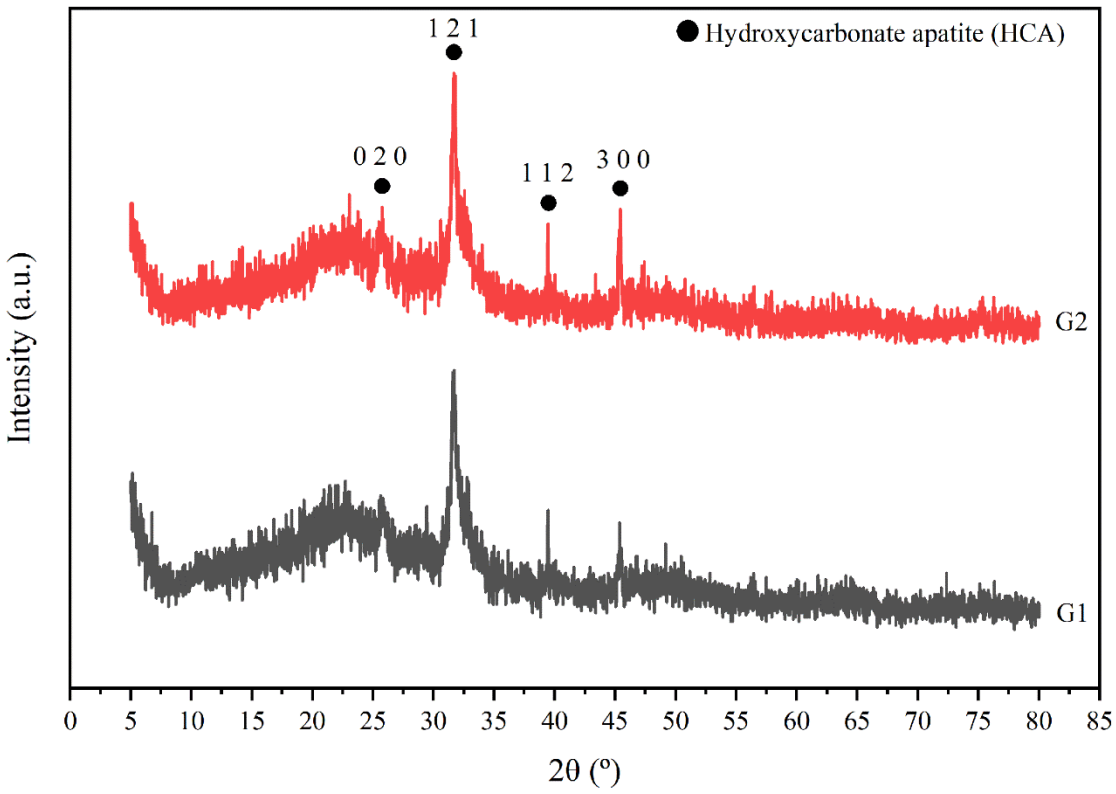

Figure 10. XRD spectra of G1 and G2 glasses after 7 days in SBF

4. Conclusions

In conclusion, the most remarkably fact is that the present study has demonstrated the feasibility of producing bioactive glasses from solution precursors using only microwave technology, consuming lower amounts of energy and less time compared to more common conventional methods such as hydrothermal synthesis and sol-gel method. Results highlighted the critical influence of pressure, used in the microwave digestor, on the material's properties and composition. Higher pressures (35 bar) corresponded to lower nitrate content, which in

turn, reduced the processing temperature (600 ^{o}C) required in the second synthesis step. This pressure-dependent relationship presents an opportunity to fine-tune the properties of bioactive glasses, which can be advantageous in tailoring their performance for specific applications.

Moreover, we found that the composition and properties of the glasses produced through the proposed procedure (digestor + microwave furnace) closely resemble those of the nominal 58S bioactive glass synthesised via the sol-gel method, confirming the efficacy of the microwave technology in yielding glass materials with the desired characteristics while significantly total reduction in energy (W) and time consumption (h) by 76% and 99% respectively (1000 W and approximately 1h for microwave digestor + microwave furnace vs 4200 W and approximately 125 h for oven + furnace).

Furthermore, the glasses exhibited a positive reaction with Simulated Body Fluid (SBF), a promising sign of their bioactivity. The potential for enhancing this reaction by extending the stabilisation period opens up ways for optimising the performance of these bioactive glasses in biological and medical applications, further underscoring the significance of our findings.

More work is already in progress in order to study the effect of higher dwelltimes for the stabilisation process as well as to validate this novel methodology in the synthesis of other bioactive glass compositions with and without dopants.

Acknowledgements
The authors of the present work thank Universitat Jaume I of Castellón the support provided in funding action 1.1. (ref. MULTIBIO/UJI-B2020-34) of the Research Promotion Plan, and the Spanish Ministry of Universities the support provided by the Margarita Salas postdoctoral contract (MGS/2022/20) financed by the European Union – NextGenerationEU.

References

[1] V. Miguez-Pacheco, L.L. Hench, A.R. Boccaccini, Bioactive glasses beyond bone and teeth: Emerging applications in contact with soft tissues, Acta Biomater 13 (2015) 1–15. https://doi.org/10.1016/J.ACTBIO.2014.11.004.

[2] J.R. Jones, Alexis. Clare, Bio-glasses : an introduction, Wiley, 2012.

[3] J.A. Juhasz, S.M. Best, Bioactive ceramics: processing, structures and properties, Journal of Materials Science 2011 47:2 47 (2011) 610–624. https://doi.org/10.1007/S10853-011-6063-X.

[4] P. Sepulveda, J.R. Jones, L.L. Hench, In vitro dissolution of melt-derived 45S5 and sol-gel derived 58S bioactive glasses, J Biomed Mater Res 61 (2002) 301–311. https://doi.org/10.1002/JBM.10207.

[5] A. Lucas-Girot, F.Z. Mezahi, M. Mami, H. Oudadesse, A. Harabi, M. Le Floch, Sol–gel synthesis of a new composition of bioactive glass in the quaternary system SiO2–CaO–Na2O–P2O5: Comparison with melting method, J Non Cryst Solids 357 (2011) 3322–3327. https://doi.org/10.1016/J.JNONCRYSOL.2011.06.002.

[6] L.L. Hench, The story of Bioglass®, in: J Mater Sci Mater Med, 2006: pp. 967–978. https://doi.org/10.1007/s10856-006-0432-z.

[7] T. Liu, D. Lai, X. Feng, H. Zhu, J. Chen, Synthesis and characterization of a novel mesoporous bioactive glass/hydroxyapatite nanocomposite, Mater Lett 92 (2013) 444–447. https://doi.org/10.1016/J.MATLET.2012.10.084.

[8] A.T. Shah, Q. Ain, A.A. Chaudhry, A.F. Khan, B. Iqbal, S. Ahmad, S.A. Siddiqi, I. ur Rehman, A study of the effect of precursors on physical and biological properties of mesoporous bioactive glass, J Mater Sci 50 (2015) 1794–1804. https://doi.org/10.1007/S10853-014-8742-X/FIGURES/9.

[9] B.T. Hoa, H.T.T. Hoa, N.A. Tien, N.H.D. Khang, E. V. Guseva, T.A. Tuan, B.X. Vuong, Green synthesis of bioactive glass 70SiO2-30CaO by hydrothermal method, Mater Lett 274 (2020) 128032. https://doi.org/10.1016/J.MATLET.2020.128032.

[10] T.A. Tuan, E. V Guseva, N.A. Tien, H.T. Dat, B.X. Vuong, A. Tien, T. Dat, H.; Vuong, C. Helmut, Z. Aleksej, Simple and Acid-Free Hydrothermal Synthesis of Bioactive Glass 58SiO2-33CaO-9P2O5 (wt%), Crystals 2021, Vol. 11, Page 283 11 (2021) 283. https://doi.org/10.3390/CRYST11030283.

[11] G. Yang, S.J. Park, Conventional and Microwave Hydrothermal Synthesis and Application of Functional Materials: A Review, Materials 2019, Vol. 12, Page 1177 12 (2019) 1177. https://doi.org/10.3390/MA12071177.

[12] A. Borrell, M.D. Salvador, A. Borrell, M.D. Salvador, Advanced Ceramic Materials Sintered by Microwave Technology, Sintering Technology - Method and Application (2018). https://doi.org/10.5772/INTECHOPEN.78831.

[13] C. Singh, V. Khanna, S. Singh, Sustainability of microwave heating in materials processing technologies, Mater Today Proc 73 (2023) 241–248. https://doi.org/10.1016/J.MATPR.2022.07.216.

[14] M. Nüchter, B. Ondruschka, W. Bonrath, A. Gum, Microwave assisted synthesis – a critical technology overview, Green Chemistry 6 (2004) 128–141. https://doi.org/10.1039/B310502D.

[15] S. Das, A.K. Mukhopadhyay, S. Datta, D. Basu, Prospects of microwave processing: An overview, Bull. Mater. Sci 32 (2009) 1–13.

[16] M. Ebrahimi, S. Manafi, F. Sharifianjazi, The effect of Ag2O and MgO dopants on the bioactivity, biocompatibility, and antibacterial properties of 58S bioactive glass synthesized by the sol-gel method, J Non Cryst Solids 606 (2023) 122189. https://doi.org/10.1016/J.JNONCRYSOL.2023.122189.

[17] L. Ji, W. Qiao, K. Huang, Y. Zhang, H. Wu, S. Miao, H. Liu, Y. Dong, A. Zhu, D. Qiu, Synthesis of nanosized 58S bioactive glass particles by a three-dimensional ordered macroporous carbon template, Materials Science and Engineering: C 75 (2017) 590–595. https://doi.org/10.1016/J.MSEC.2017.02.107.

[18] A. Moghanian, S. Firoozi, M. Tahriri, Characterization, in vitro bioactivity and biological studies of sol-gel synthesized SrO substituted 58S bioactive glass, Ceram Int 43 (2017) 14880–14890. https://doi.org/10.1016/J.CERAMINT.2017.08.004.

[19] M. Menning, M.A. Aegerter, Sol-gel technologies for glass producers and users , Kluwer Academic Publishers, Boston, 2004.

[20] R. Benavente, M.D. Salvador, O. García-Moreno, F.L. Peñaranda-Foix, J.M. Catalá-Civera, A. Borrell, Microwave, Spark Plasma and Conventional Sintering to Obtain Controlled Thermal Expansion β-Eucryptite Materials, Int J Appl Ceram Technol 12 (2015) E187–E193. https://doi.org/10.1111/IJAC.12285.

[21] A.L.B. Maçon, T.B. Kim, E.M. Valliant, K. Goetschius, R.K. Brow, D.E. Day, A. Hoppe, A.R. Boccaccini, I.Y. Kim, C. Ohtsuki, T. Kokubo, A. Osaka, M. Vallet-Regí, D. Arcos, L. Fraile, A.J. Salinas, A. V. Teixeira, Y. Vueva, R.M. Almeida, M. Miola, C. Vitale-Brovarone, E. Verné, W. Höland, J.R. Jones, A unified in vitro evaluation for apatite-forming ability of bioactive glasses and their variants, J Mater Sci Mater Med 26 (2015) 1–10. https://doi.org/10.1007/S10856-015-5403-9/FIGURES/5.

[22] T. Kokubo, H. Takadama, How useful is SBF in predicting in vivo bone bioactivity?, Biomaterials 27 (2006) 2907–2915. https://doi.org/10.1016/J.BIOMATERIALS.2006.01.017.

[23] A.L.B. Maçon, S. Lee, G. Poologasundarampillai, T. Kasuga, J.R. Jones, Synthesis and dissolution behaviour of CaO/SrO-containing sol–gel-derived 58S glasses, J Mater Sci 52 (2017) 8858–8870. https://doi.org/10.1007/S10853-017-0869-0/FIGURES/7.

[24] E. Cañas, O. Rojas, M.J. Orts, H. Ageorges, E. Sánchez, Effect of feedstock and plasma gun on the microstructure and bioactivity of plasma sprayed bioactive glass coatings, Surf Coat Technol 406 (2021) 126704. https://doi.org/10.1016/J.SURFCOAT.2020.126704.

[25] P. Sepulveda, J.R. Jones, L.L. Hench, Characterization of melt-derived 45S5 and sol-gel–derived 58S bioactive glasses, J Biomed Mater Res 58 (2001) 734–740. https://doi.org/10.1002/JBM.10026.

[26] H. Aguiar, J. Serra, P. González, B. León, Structural study of sol–gel silicate glasses by IR and Raman spectroscopies, J Non Cryst Solids 355 (2009) 475–480. https://doi.org/10.1016/J.JNONCRYSOL.2009.01.010.

[27] A. Balamurugan, G. Sockalingum, J. Michel, J. Fauré, V. Banchet, L. Wortham, S. Bouthors, D. Laurent-Maquin, G. Balossier, Synthesis and characterisation of sol gel derived bioactive glass for biomedical applications, Mater Lett 60 (2006) 3752–3757. https://doi.org/10.1016/J.MATLET.2006.03.102.

[28] E. Krishnamoorthy, V. Sugumaran, R. Gosala, B. Purushothaman, B. Subramanian, Influence of varying thermal treatment on bioactive material with equal Ca/P ratio: A local drug delivery system for bone regeneration, J Biomed Mater Res B Appl Biomater 111 (2023) 402–415. https://doi.org/https://doi.org/10.1002/jbm.b.35159.

[29] D. Durgalakshmi, R.A. Rakkesh, S. Balakumar, Stacked Bioglass/TiO2 nanocoatings on titanium substrate for enhanced osseointegration and its electrochemical corrosion studies, Appl Surf Sci 349 (2015) 561–569. https://doi.org/https://doi.org/10.1016/j.apsusc.2015.04.142.

[30] V. Sugumaran, E. Krishnamoorthy, A. Kamalakkannan, R.C. Ramachandran, B. Subramanian, Unscrambling the Influence of Sodium Cation on the Structure, Bioactivity, and Erythrocyte Compatibility of 45S5 Bioactive Glass, ACS Appl Bio Mater 5 (2022) 1576–1590. https://doi.org/10.1021/acsabm.1c01322.